Egyptian Geophysical Society
EGS Journal, Vol. 18, No. 1, 69-82 (2020)

RELATION BETWEEN SPECTRAL INDUCED POLARIZATION (SIP) AND WATER SATURATION OF TAREF SANDSTONE, WESTERN DESERT, EGYPT

A. ELSHENAWY(1)*, M. MABROUK*(1)*, A. YOUSSEF*(1)*, S. MOUSA*(2)*,*
K. FARAG(2) *and P. SOUPIOS*(3)

(1) Geophysics Department, Desert Research Centre (DRC), Cairo, Egypt
(2) Geophysics Department, Faculty of Science, Ain Shams University, Cairo, Egypt
(3) Department of Geosciences, King Fahd University of Petroleum and
Minerals-KFUPM, Dhahran, Saudi Arabia

العلاقة بين الاستقطاب الطيفي المستحث (SIP) و التشبع للحجر الرملي (طارف)، الصحراء الغربية، مصر

الخلاصة: شهد العقد الماضى اهتماماً متزايداً بتطبيق طريقة الاستقطاب الطيفى المستحث (SIP) فى التطبيقات الهيدروجيولوجية والبيئية. ويعد المحرك الرئيسى لهذا هو حقيقة أن كلا من المياه الجوفية والتيار الكهربائى يتحركان عبر مسارات مترابطة عبر المصفوفة الصخرية. ومع ذلك، فإن تطبيق أسلوب SIP فى دراسات منطقة الفادوز (النطاق غير المشبع فوق منسوب سطح المياه) لم يحظ إلا بقدر ضئيل من الاهتمام، وتركز النماذج الخاصة بآلياتها فى مواد الأرض بشكل أساسى على المواد المشبعة بالمياه. لذلك، من الواضح أن معلاغة اعتماد معاملات الأطياف الكهربائية على التشبع ضرورى لتفسير قياسات SIP بشكل موثوق فى منطقة الفادوز. تحاول هذه الدراسة أن تضيف إلى معرفة تأثير تشبع الماء فى نطاق الفادوز الذى يعلو منسوب سطح الماء الأرضى على التيار الكهربائي ومعاملاته على عينات الحجر الرملي الكامل المشبعة بالكامل في منطقة طارف (الصحراء الغربية ، مصر). حيث تم رصد ظواهر واضحة لنوع الاسترخاء في حالة التشبع الكامل لجميع عينات الحجر الرملي في هذه الدراسة، واعتماد واضح لمعلمات SIP على تشبع الماء بشكل عام، يعتمد الجزء الحقيقي من التوصيلية الكهربائية بشكل أساسي على التوصلية المشبعة وكذلك مسامية الصخر ، حيث يكون لخصائص الطبقة الكهربائية المزدوجة على سطح السائل تأثير كبير على الجزء التخيلي. كما لوحظ أيضا زيادة في المقاومة وانخفاض في التوصيلية الكهربائية الحقيقية مع تقليل التشبع ؛ وقد لوحظ بوضوح السلوك غير الخطي لكل من زاوية الطور وكذلك التوصيلية التربيعية مع التشبع. علاوة على ذلك ، أظهرت الدراسة هيمنة لنقطتي انعكاس لتشبع الماء على سلوك الأطياف الانتخابية مع تغيير التشبع على العينات المدروسة. أخيرا أكدت الدراسة الاعتماد القوي لمعاملات SIP على تشبع الماء والقيمة المحتملة لتطبيق لطريقة SIP في نمذجة المياه الجوفية وكذلك دراسات تلوث المياه الجوفية بسبب أحجام مسام الحلق وتأثير التوزيع على سلوك الاسترخاء.

ABSTRACT: *The last decade witnesses a growing interest in the application of the Spectral Induced Polarization (SIP) method in hydrogeological and environmental investigations. This is may be inspired by the fact that both groundwater and electrical current move via interconnected paths through rock matrix. However, application of the SIP method in vadose zone studied has received minimal attention, and models for its mechanisms in Earth material primarily focus on water-saturated materials. Therefore, knowing the dependence of electrical spectra parameters on saturation is clearly necessary in order to reliably interpret SIP measurements in vadose zone. This paper tries to add to the knowledge of the effect of water saturation on A.C. electrical current and its parameters on fully and partially saturated Taref sandstone samples (Western desert, Egypt). All of the sandstone samples under this study displayed clear relaxation type phenomena at fully saturation status, and an obvious dependence of SIP parameters on water saturation. Generally, the real part of the conductivity depends mainly on the saturating fluid conductivity as well as porosity of the rock, where the characteristics of the electrical double layer at the matrix-fluid interface have the major influence on the imaginary part. An increase in resistivity and a reduction in real conductivity with reducing saturation were noticed; where a non-linear behavior of both phase angle as well as quadrature conductivity with saturation is clearly observed. Moreover, two water saturation reflection points seem to dominate the electoral spectra behavior with changing saturation over the studied samples. The strong dependence of SIP parameters on water saturation clarified in this study, confirmed the potential value of SIP method for groundwater modeling as well as groundwater contamination studies due to pore throat sizes and distribution influence on relaxation behavior.*

1. INTRODUCTION

Recently, due to achieved advanced in geophysical instrumentation sensitivity and groundwater modelling programs, the use of geophysics in hydrologic investigations has been expanding rapidly over the past decade. These applications seek to help understand aquifer heterogeneity via the identification of spatial patterns of petrophysical parameters and relate them to hydrologic properties or states. In fact, the ability to predict reliably hydraulic properties of subsurface formations using a non-invasive tool is considered to be one of the most important and challenging goals in hydrogeophysics. Moreover, the ability to predict or assess of the spatial variability of these properties is also important for any future hydrogeological or environmental strategies. Applying conventional methods to determine these properties is still difficult, and sometimes not practical due to the inevitable disturbance of the porous media, (Kruschwitz et al., 2010). On the other hand, the ability to reliably quantify, monitor, and map key hydraulic properties using geophysical tools would result in a significant advances in subsurface hydrogeological characterization, (e.g., Kemna et al., 2004; Soupios et al., 2007; Kemna et al., 2012; Fiandaca, 2018; and Maurya et al., 2018).

Although almost all geophysical methods have been intensively applied to solve hydrogeological and environmental problems, geoelectrical methods are the mostly used and more appropriate for such problems. Moreover, among all geoelectrical methods, Induced Polarization (IP) seems to have extra potential and information than the traditional electrical methods. Where traditional electrical methods (i.e. dc-resistivity and EM induction methods) are only sensitive to the in-phase conductivity component (the ability of the Earth to transport charge via ohmic conduction currents, energy loss), the Induced Polarization (IP) technique has extra advantage as it is also sensitive to the out-of-phase conductivity (the ability of the earth to transport charge via polarization (energy storage) (Ntarlagiannis et al., 2016). Moreover, what is known as electrical spectrometry or Spectral Induced Polarization (SIP) is a measure of both real and imaginary components of the conduction of Earth materials using alternating current over a wide frequency range (mHz to KHz).

Although the huge amount of studies trying to link hydraulic and electrical properties of porous media, there are no universal models explaining such relationship. Incorporating charge storage (complex resistivity) within a petrophysical model may, however, result in more appropriate relationships between the electrical spectra and some hydrogeological parameters. This is may be due to the influence of the complex resistivity by the characteristics of the pore/grain interface. In fact, several attempts or approaches have been suggested in the last decades to link some intrinsic properties of porous rock samples such as specific surface, cation exchange capacity (CEC) to parameters extracted or determined from the shape of the electrical spectra (e.g. Klein & Sill, 1982; Börner et al., 1996; Lesmes & Morgan, 2001; Titov et al., 2002; Scott & Barker, 2003; Binley et al., 2005; Kruschwitz, 2008; Leroy et al., 2008; and Kruschwitz et al., 2010).

Prior studies have shown several correlations between hydrogeophysical characteristics of rocks and the SIP response and a series of hypotheses were proposed (Kemna et al., 2004; Titov, 2004; Ulrich and Slater, 2004; Binley et al., 2005; Scott and Barker, 2005; Scott, 2006; Ghorbani, 2007; Leroy et al., 2008; Kruschwitz et al., 2010; Joseph et al., 2015).

Moreover, there is a growing interest in the application of the induced polarization (IP) method in environmental investigations, application of the IP method in vadose zone studies (unsaturated region above the water table) which has received till now, minimal attention in the literature. Studies considering the dependence of IP parameters on saturation are still limited (Vinegar and Waxman, 1984; Worthington and Collar, 1984; Ulrich, 2005; Binley et al., 2005; Koch et al., 2011) and models for IP mechanisms in Earth material primarily focus on water-saturated materials. Therefore, the dependence of IP parameters on saturation is clearly needed to be known to reliably interpret IP measurements in terms of lithologic parameters such as grain size, specific surface area, and hydraulic conductivity where the survey is completely or partly conducted in the vadose zone.

2. GEOLOGICAL AND HYDROGEOLOGICAL DESCRIPTION

Nubia Sandstone aquifer represents the main source of groundwater in the Western desert, which constitutes about 68% of the surface area of Egypt. The study area is located in the central part of the Western Desert of Egypt.

The exposed sedimentary succession in the Dahkla area ranges from Late Cretaceous to Quaternary. Said (1990) reported that the Upper Jurassic Campanian sequence, represented by sandstone and clay, as Nubia Sandstone, which overlies directly the basement rocks. From older to younger, Nubia Sandstone is subdivided into different rock units as follows: The Six Hills, Abu Ballas, Sabaya, Maghrabi, Taref and Mut Formations, (Ghoubachi, 2001). Shata (1953) considered the Dakhla depression as a low area occurring between major structural highs. On the other hand, Hermina, et al. (1961) regarded it as a major syncline located on the north plunge of the Nubia huge upwarping, which are oriented NE-SW direction.

Awad and Ghobrial, (1965) described Taref Formation as of fine to medium grained and well sorted sandstone with a few shale interbeds overlying the Maghrabi Formation (shale and claystone) and underlies the Mut Formation (claystone), with an average thickness of more than 100m at its type locality at Gabal El-Taref in north El Kharga Oasis. Regarding its shallow depth and good water quality, Taref sandstone aquifer is considered one of the most important water bearing formations in the western desert, Gad et al. (2011).

3. ELECTRICAL SPECTROMETRY

In practice, induced polarization is measured as a change in voltage with time or frequency. The time and frequency domain IP methods are fundamentally similar. However, in the former, the decay of voltage between two potential electrodes is recorded after the cut off of the applied direct current (DC) (time domain method), where the latter uses alternating current (AC) to induce electric charges in the subsurface, and the magnitude and phase angle of the impedance is measured at different AC frequencies (frequency-domain method) (Sumner, 1976). The SIP technique measures a frequency spectrum ranging from 0.001 Hz to 10 kHz via injecting current into the ground between two electrodes and then measurements of the impedance are made between two other (potential) electrodes.

According to Ohm’s Law (equation 1), the resistance R is defined as the ratio between voltage, V, and current, I.

$$R \equiv \frac{V}{I} \tag{1}$$

The previous simple and common equation for an ideal resistor in an electric circuit has several assumptions. For example, the ideal resistor follows Ohm’s Law at all voltage and current bands, its resistance value is totally independent of frequency, and both AC current and voltage are in-phase with each other through the resistor. However, the Earth materials exhibit much more complex behaviour than an ideal resistor, such as they usually characterised by frequency dependent electrical response. Generally, resistivity ρ^* (ω), conductivity σ^* (ω), and dielectric permittivity ε are the most common used parameters in geophysics. These three parameters can be related to each other by:

$$\sigma \equiv \frac{1}{\rho*(\omega)} \equiv i\omega\varepsilon * (\omega) \tag{2}$$

Where $i = \sqrt{-1}$, is the relationship between angular ω (expressed in radians/second), and *f* frequency (expressed in hertz) is $\omega=2\pi f$.

According to Slater (2007), each of three previously mentioned parameters contains a total energy loss term (conduction), and a total energy storage term (polarization). The real (in-phase) conductivity σ' is the property defining the ability of the Earth material to transport charge via ohmic conduction current (energy loss), where the imaginary (out-of-phase) conduction σ'' is defining the ability of the Earth material to transport charge via polarization (energy storage). Where the DC resistivity can detect the real conductivity, the imaginary or quadratic conductivity can be quantified with IP or SIP techniques.

In general, the term impedance “Z “is usually used instead of resistance for AC circuits. Impedance could be regarded as a measure of the ability of a material to resist the flow of AC current. Impedance is normally measured using a small excitation current signal, and the output voltage measured at any frequency will induce a phase lag (phase shift) relative to the excitation current (Figure 1). This output voltage is equal to the vector sum of both real (in-phase) and imaginary (out-of-phase) components. Therefore, the Earth materials electrical properties can be expressed as a complex number where both the magnitude ($|\sigma|=\sqrt{(\sigma')^2+(\sigma'')^2}$) and phase lag ($\theta = \tan^{-1} (\sigma''/\sigma')$), (Binley and Kemna, 2005; and Kemna et al., 2012).

As illustrated in figure (2), the current response to a sinusoidal potential will be a sinusoid at the same frequency but shifted in phase, which can be expressed by a negative phase angle as follows:

$$I(t) = I_0 \sin(\omega t) \tag{3}$$

$$V(t) = V_0 \sin(\omega t + \theta) \tag{4}$$

Where $I(t)$ and $V(t)$ are the current and potential at time t, respectively, and I_0 and V_0 are the amplitude of the current and potential signal. Similar to equation (1) for DC, the complex impedance Z^* (ω), or its reciprocal admittance Y^* (ω) for AC circuit could be calculated as:

$$Z = V(t)/I(t) = 1/Y \tag{5}$$

Several methods can be employed in order to display theses parameters graphically. The common method of representing complex electrical parameters is to split them into their real and imaginary components, and then plot each of them separately against frequency.

4. SPECTRAL INDUCED POLARIZATION (SIP)

Spectral induced polarization (SIP) is considered as an extension of frequency induced polarization, where the resistivity magnitude as well as its phase with respect to the current is measured over a wide frequency spectrum (typically in the mHz to kHz range) instead of using only two frequencies, (Figure1). According to Kemna (2000), if the input current is a square wave, the complex resistivity signal will be the phase angle between the fundamental harmonic of the transmitted and received signals, where the phase angle is the one whose tangent is the ratio between the imaginary and real components of the measured resistivity and is expressed as:

$$\theta=\tan^{-1}(\rho''/\rho') \tag{6}$$

The magnitude of the complex resistivity is determined from the real and imaginary components of the above mentioned parameters and is expressed as:

$$(|\rho|=\sqrt{(\rho')^2+(\rho'')^2} \tag{7}$$

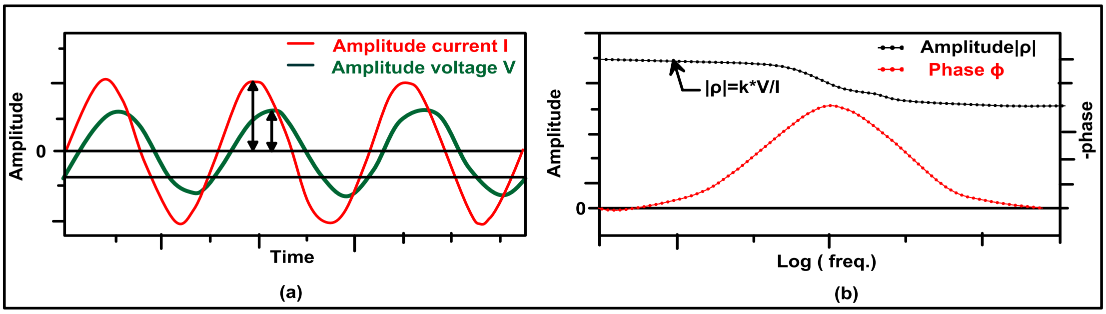

Figure (1): Data acquisition in Spectral Induced Polarization SIP. (a) A sinusoidal electrical current *I* the resulting voltage *V* is measured. The measured voltage is characterized by a phase lag in time relative to the excitation current. (b) Resistivity magnitude (amplitude) and phase angle of the electrical spectrum, (Ghorbani, 2007).

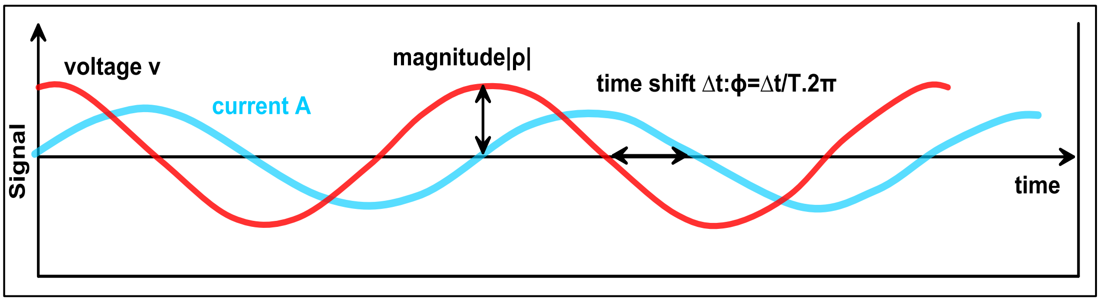

Figure (2): Complex resistivity signal for a distinct frequency. The applied voltage (V) causes a subsequent current (A) signal, which is shifted in time. (Kruschwitz, 2007).

5. ORIGIN OF INDUCED POLARIZATION

The electrical polarization behavior of multi-phase porous media, including porous rocks, is believed to be a result of additive or integrated processes, where electrical fields form around the solid phase in addition to those arising through the electrolytic liquid phase. For fluid saturated geological materials, which consist of a mixture of grains and fluids, each with different electrical conductivity, give rise to some of the observed polarization effects. In addition, the environment in the immediate vicinity of the grain-solution interface, where an electrochemical double layer (EDL) exists, is believed to cause an excess conduction and significant polarization effect (Chelidze and Gueguen, 1999; Lesmes and Morgan 2001; Scott and Barker 2005; Leroy et al., 2008; Revil, 2012).

5.1. Electrochemical Double Layer (EDL)

The EDL is the name given to describe the structure that appears in any region between two different phases, where the development of a net charge on the surface of an object (a solid particle, a liquid droplet, a gas bubble, or a porous body) when it is placed into a liquid creates an ion concentration gradient in the solution. In saturated porous media (e.g. sandstones), this region is the area between the grain surface (where we have a charged surface) and the bulk of the aqueous environment or electrolyte (where a balancing counter charge will occur in). The balancing counter charge process will not produce uniformly distributed charges throughout the liquid phase, but there will be an increased concentration of counter ions close to the charged surface. In saturated porous media, as the grain surface usually carries excess negative ions, it attracts cations to it to restore electroneutrality forming what is known as the EDL (Grahame 1952; Chelidze and Gueguen 1999; Lesmes and Morgan 2001; Reppert et al 2001; Leroy et al., 2008; Revil, 2012), (Figure 3).

The movement of ions in the Stern and/or the diffuse layer during and after the application of external electrical field is considered as one of the main contributions to the observed low frequency electrical response of porous Earth materials. In the Stern layer, where ions are capable of moving only tangentially along the surface of the particle, a simple model for a dilute suspension of spherical, colloidal particles in a conducting electrolyte is generally used to describe this movement, which is characterized by both in-phase and quadrature conductivity components. A simple model for the relaxation of the Stern layer was proposed by Schwarz (1962) producing a single Debye relaxation time τ_s given by,

$$\tau_s = R^2/2D_s \qquad (8)$$

Where, *R* is the particle radius and D_s is the diffusion coefficient of the ions in the Stern layer. Later, Schurr (1964) generalized this model by including the effects of DC surface conductivity.

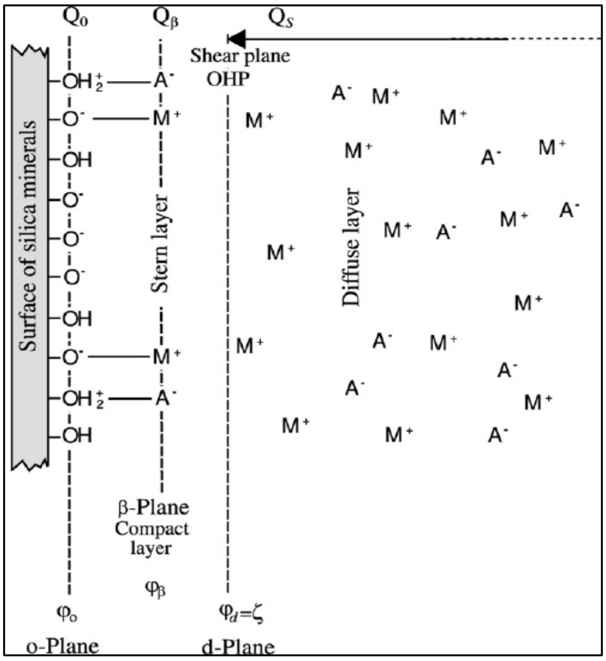

Figure (3): Sketch of the electrical triple-layer. M represents the metal cations and A the anions. OHP represents the outer Helmholtz plane. Q_0 is the surface charge density of the surface of the mineral, Q_β is the surface charge density of the Stern layer, and Q_S is the equivalent surface charge density of the diffuse layer (Leroy and Revil 2006; Leroy et al., 2008).

On the other hand, several models have been adopted for the polarization of the diffuse layer (e. g. Dukhin and Shilov, 1974; Fixman 1980; De Lima and Sharma, 1992; Chelidze and Gueguen, 1999) which generally supersede the Schwarz (1962) model. In general, these models for the diffuse layer polarization produce a polarization that is broader than the Schwarz model Debye relaxation.

5.2. Membrane (electrolytic) polarization:

The term membrane (electrolytic) polarization refers to the type of the IP effects that are observed during the absence of metallic type minerals in the ground. The following two mechanisms are believed to be the main cause of membrane or electrolytic polarization:-

A- Constriction within a pore channel:

According to Sumner (1976), the rock surface is covered by a net negative charge which attracts opposite charges within the pore fluid forming a positively charged (Figure 4). When the diameter of the pore channel is reduced to less than this distance, the mobile ions can block pore passage and will accumulate and increase their concentration around these constricted zones during the applied voltage. After the applied voltage is switched off, the ions will diffuse slowly returning to equilibrium producing the measured IP response.

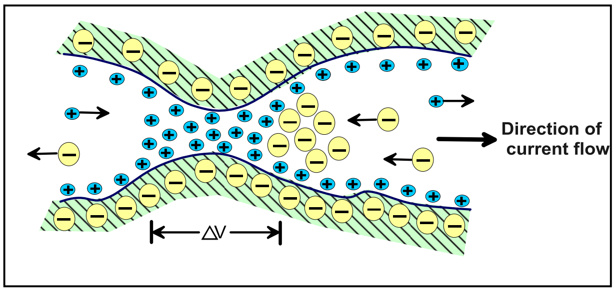

Figure (4): Membrane polarization associated with constriction between mineral grains (Reynolds, 1997).

B- Presence of clay particles:

As the surface of clay particle is negatively charged, it attracts positive ions from the electrolytes present in the capillaries of clay aggregate, forming an electrical double layer at the surface of the particle. The positively charged zone at the surface of the clay particle will repel other ions with the similar charge impeding their movement through the capillaries and causing imbalance in the ion concentration forming a double layer. The displaced positive ions (during applied voltage) will redistribute themselves in their former equilibrium pattern after the interruption of the current. This process of redistribution causes a decaying voltage and is considered responsible for the measured IP effect of clay deposits (Kiberu, 2002; Bücker et al., 2017).

6. RELAXATION MODELS

A quantitative description model is necessary to characterize the frequency dependence of the electrical properties of the matter. A review of existing approaches is given in Pelton et al (1983), Ruffet et al., (1991a), and Dias (2000). Although the main origin of the relaxation phenomena is not completely understood, and even some of these models are empirical and lack to theoretical physical justification (Jonscher, 1975; Ruffet et al., 1991b), they still very practicable for their ability to relate descriptive petrophysical parameters of rocks to measurable spectral quantities.

All mathematical models that have been used to describe the relaxation phenomena have similar features: a low frequency asymptote, a dispersive region and a high frequency asymptote. The dispersive region is considered to be centered around a typical frequency, which can be related to a particular relaxation time, τ (Kruschwitz, 2008).

6.1. Debye Relaxation Model:

This model represents the simplest form of relaxation, (Figure 5). A polarisation with a single relaxation time, τ, and an exponential decay can be characterised by a classic Debye relaxation (Pelton et al., 1978a):

$$\varepsilon^{*} = \varepsilon_{\infty} + \frac{(\varepsilon_{s} - \varepsilon_{\infty})}{(1 + \imath\omega\tau)} - \imath\frac{\sigma_{s}}{\omega} \tag{9}$$

This has a maximum energy dissipation, or out-of-phase response, at a critical frequency $f_c = 1/2\pi\tau$, where ε_s and ε_∞ are the permittivity at $f<<f_c$ and $f>>f_c$ respectively, and σ_s is the ohmic conductivity, often taken to be the direct current conductivity, σ_{DC}.

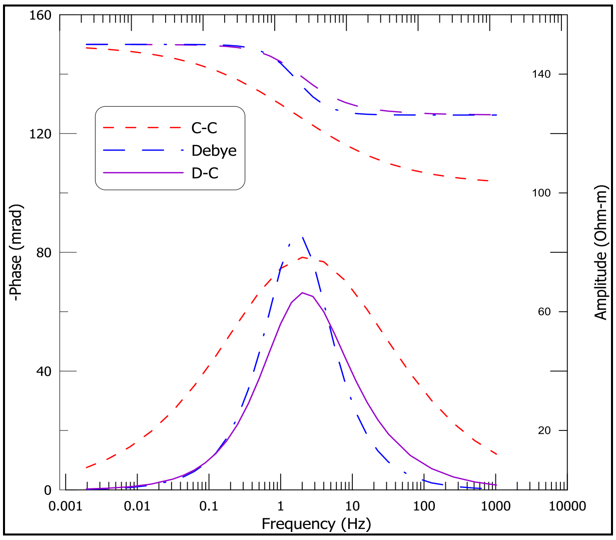

Figure (5): Comparison of Debye, Davison Cole and Cole-Cole relaxation models.

6.2. Cole-Cole Family Models

An important modification to the Debye model was suggested by Cole and Cole, (1941), and later adopted by Pelton et al., (1978a) to describe complex resistivity spectra of mineralized rocks over the frequency range 10 mHz to 10 kHz, (Fiandaca et al., 2018). As shown in Figure (5), a broadening of the response function can be described by the sum of many relaxation times with a log normal distribution according to the Cole-Cole model:

$$\varepsilon^{*} = \varepsilon_{\infty} + \frac{(\varepsilon_{s} - \varepsilon_{\infty})}{(1 + \imath\omega\tau)^{1-\alpha}} - \imath\frac{\sigma_{s}}{\omega} \tag{10}$$

Where α is the distribution function exponent. Additional exponents can be added to make the function asymmetrical. Following Pelton et al., (1983) the complex electrical behavior of most earth materials can be best described using modified Cole-Cole like impedance models. Figure 5 shows comparison of Debye, Davison Cole and Cole-Cole relaxation models. The common expression forms of the Cole-Cole family models are listed in the table. The most general model is the generalized Cole-Cole model, and all others are simplifications or special cases, where, the model parameter c is a dimensionless exponent and gives the slope of the left (or right -c) hand side of the phase spectrum in a double logarithmic plot, and *m* is the chargeability corresponding to the polarization immediately after the switch off of the harmonic electrical field (Kruschwitz, 2008).

For example, the standard Cole-Cole model achieved if a=1, where in Davison-Cole model c=1. If both (a and c) equal to 1, the model will simplified to Debye model, (Figures 6 & 7).

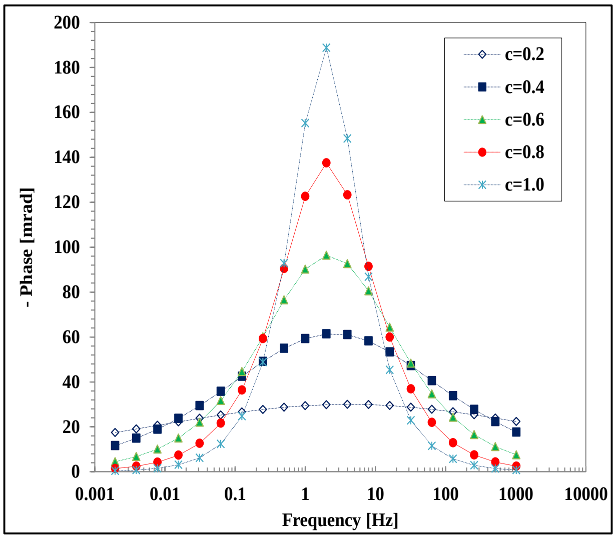

Figure (6): Illustration of the effect of changing the exponent (c) value on the phase spectra.

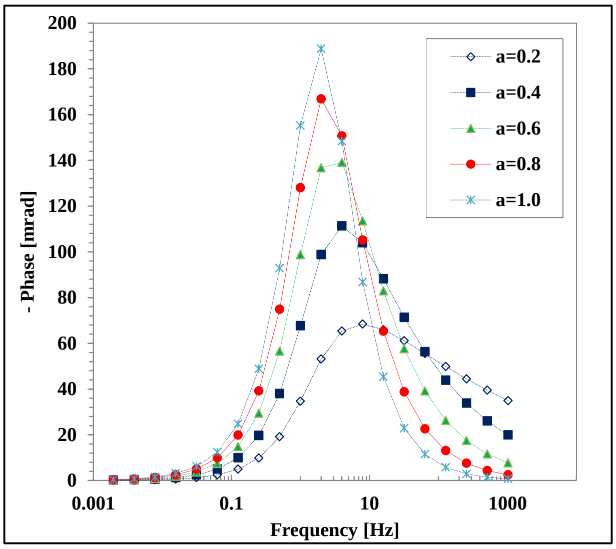

Figure (7): Illustration of the effect of changing the exponent (a) value on the phase spectra.

Table: Overview of simple relaxation models. The last two columns indicate the low and high frequency phase angle asymptotic slopes (after Kruschwitz, 2008).

Name	**Model function**	***ω→0***	***ω→ ∞***
Debye	$R = 1 - m\left[1 - \left(\frac{1}{1+(i\,\omega\tau)}\right)\right]$	1	1
Warburg	$R = 1 - m\left[1 - \left(\frac{1}{1+(i\,\omega\tau)^{1/2}}\right)\right]$	0.5	-0.5
Cole-Cole	$R = 1 - m\left[1 - \left(\frac{1}{1+(i\,\omega\tau)^{c}}\right)\right]$	c	$-c$
Generalized Cole-Cole	$R = 1 - m\left[1 - \left(\frac{1}{\left(1+(i\,\omega\tau)^{c}\right)^{a}}\right)\right]$	c	$-a\,c$

7. EXPERIMENTAL PROCEDURES

One of the most important and usually difficult tasks to obtain accurate SIP measurements in the laboratory is to exclude and/or remove any external effect or response caused by the measuring system, in order to be sure that the measured spectra are due to changes happened entirely to the examined sample. The most common reasons for errors or noise of SIP measurements at low frequencies are what is known as electrode polarization. Electrode polarization is formed due to a build-up of charge on the potential measuring electrodes during the SIP measurements, where the conduction mechanism changes from electronic (in the measuring electrodes), to electrolytic (in the solution). On the other hand, at high frequencies, there will be electromagnetic coupling between the connecting wires and the measuring cell, which causes an out of phase component to be added to the measurements.

A programme of laboratory measurements was performed to measure the SIP response of sandstone samples over different saturation levels. The measurements have been made using the arrangement outlined by Gomaa (2009), where thin Taref sandstone samples of thickness 6 mm and diameter 37 mm were prepared. A four non-polarizing Cu/CuSO4 gel electrodes system was used in the measurements as shown in Figure (8). Both current and potential electrodes are immersed in an agar-agar/copper sulphate gel compartment providing a good electrical connection between the current/potential electrodes and the sample, and avoiding any penetration and contamination of the sample porous material, so it cannot alter the electrical properties of the sample with time. The Hioki 3522- 50 LCR Hitester Impedance analyzer connected to the non-polarizing electrodes system used to measure the electrical spectrometry of the fully and partially saturated sandstone samples in the form of the resistivity magnitude and phase spectra over the used range.

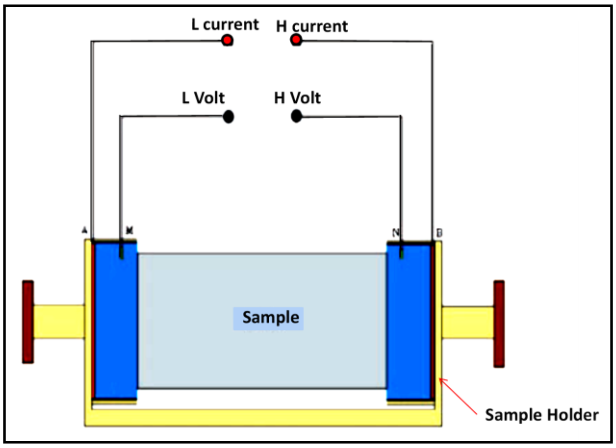

Figure (8): Schematic diagram of the non-polarizing Cu/CuSO4 gel electrodes (Gomaa, 2009).

No signs of the polarization effects were observed in the measured fluid spectrum. On the other hand, the higher frequency coupling effect still observed throughout experiments, indicating that this effect is not caused by the rock samples. Moreover, to demonstrate repeatability, every sample measurement was repeated, the average measured complex electrical parameters were calculated. For simplicity, only the average values will be shown.

Each sample was placed in a small jar inside a bell jar which was pumped for 15 minutes to ensure the sandstone was fully evacuated. The saturation fluid (0.01 M NaCl solution) was added to the small jar to fully submerge the sample and left for 15 minutes in the vacuum to allow complete saturation. Each sample was weighted before and after the saturation process to allow calculation of porosity and ensure complete saturation had been achieved. The saturated samples were left submerged in the saturation fluid for 24 hours in the incubator to allow the test temperature of 25˚C to be reached. Subsequent measurements with the determination of weight were made while the sample was let to dry. Measurements were made during drainage rather than imbibition (Ulrich and Slater 2004). Saturation levels were calculated as:

$$S_w=[(S_w – S_d)/S_d]\times 100 \qquad (11)$$

Where, S_w = water saturation (%), S_w = wet sample weight, S_d = dry sample weight. Every sample measurement was repeated; the average measured complex electrical parameters were calculated. For simplicity, only the average values will be shown.

8. RESULTS

The calculated bulk density of the sandstone samples (T1-T4) ranges from 1.89 gm/cm^3 to 2.24 gm/cm^3 and their mean value is 2.0 gm/cm^3. On the other hand, the measured grain density ranges from 2.63 gm/cm^3 to 2.68 gm/cm^3 and of a mean value is 2.65 gm/cm^3 indicating that quartz is the main mineralogical composition of these samples. Total porosity was found to be between 20.6 % and 29 % and their mean value is 25 %, where the effective porosity ranges from 17 % to 24 %, with a mean value of 20.3%.

Within the mHz to kHz frequency range, which the conductivity is measured over, all of the four sandstone samples displayed clear relaxation type phenomena at fully saturation status. These spectra results displayed here have been expressed in both Polar and Cartesian form. In the Polar form, the complex conductivity is expressed in terms of a magnitude (|σ|) and a phase (φ). On the other hand, in the Cartesian form, the complex conductivity is expressed by the in-phase or real (σ') and the quadrature or imaginary (σ") components. Besides, the absence of Warburg impedance rises at low frequencies clarify that there is no relevant electrode polarization, suggesting the use of CuSO4 gel electrodes almost eliminate the electrode polarization impedance, similar to the findings of by Gomaa (2009).

Figures (9-12) show the measured SIP parameters at different saturation levels (seven levels). In general, the SIP response of a polarized porous material is characterized by a decrease in resistivity magnitude as the frequency increased throughout the spectrum. On the other hand, a peak is shown in the phase spectra at the lower end of the spectrum and a rise in phase angle at higher frequencies which is attributed to coupling effects (Figures 9-12, b). similarly in the Cartesian form, a positive peak in the quadrature conductivity spectra is noticed, which is also associated with a decrease in the in-phase conductivity over the measure frequency range,

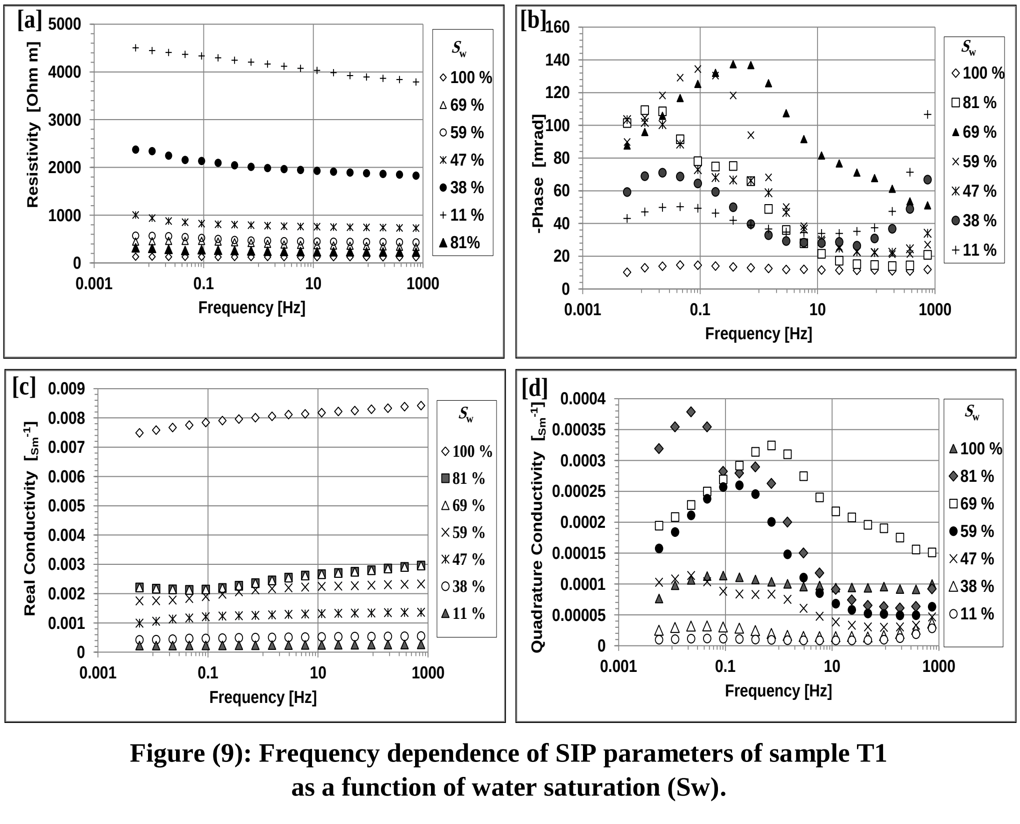

Figure (9): Frequency dependence of SIP parameters of sample T1 as a function of water saturation (Sw).

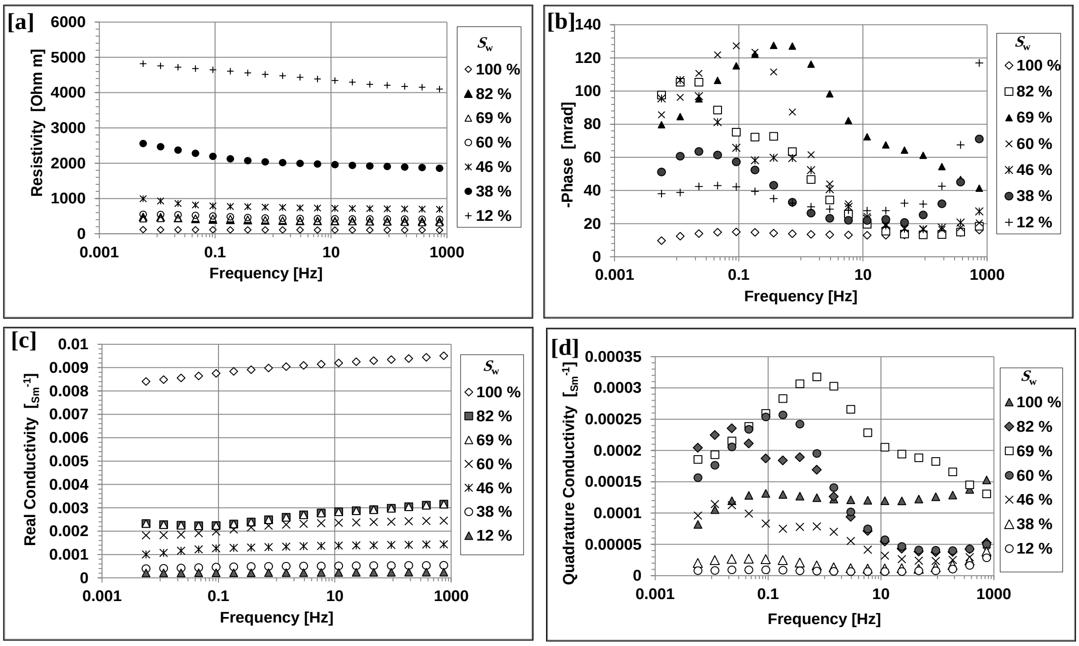

Figure (10): Frequency dependence of SIP parameters of sample T2 as a function of water saturation (Sw).

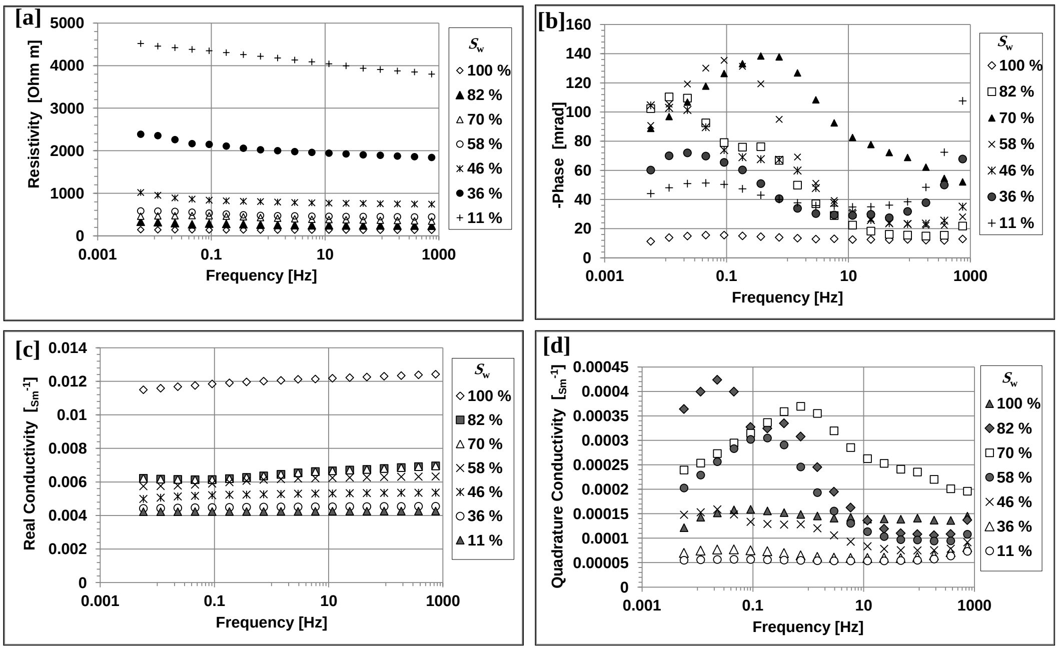

Figure (11): Frequency dependence of SIP parameters of sample T3 as a function of water saturation (Sw).

where the frequency at which the maximum rate of decrease of the in-phase conductivity occurs is at the same frequency as the quadrature conductivity peak (Figures 9-12, c&d).

Figures (9-12, a&c) show weak frequency dependence of both bulk resistivity and real conductivity with reducing water saturation. On the other hand, Figures (9:12, b&d) exhibit strong and complicated frequency dependence of phase angle as well as quadrature conductivity with changing water saturation.

On the other hand, Figure (13) shows the dependence of SIP parameters on water saturation. The four measured SIP parameters (at 1.4 Hz) of the four Taref sandstone samples (T1-T4) plotted against frequency at the seven saturation levels.

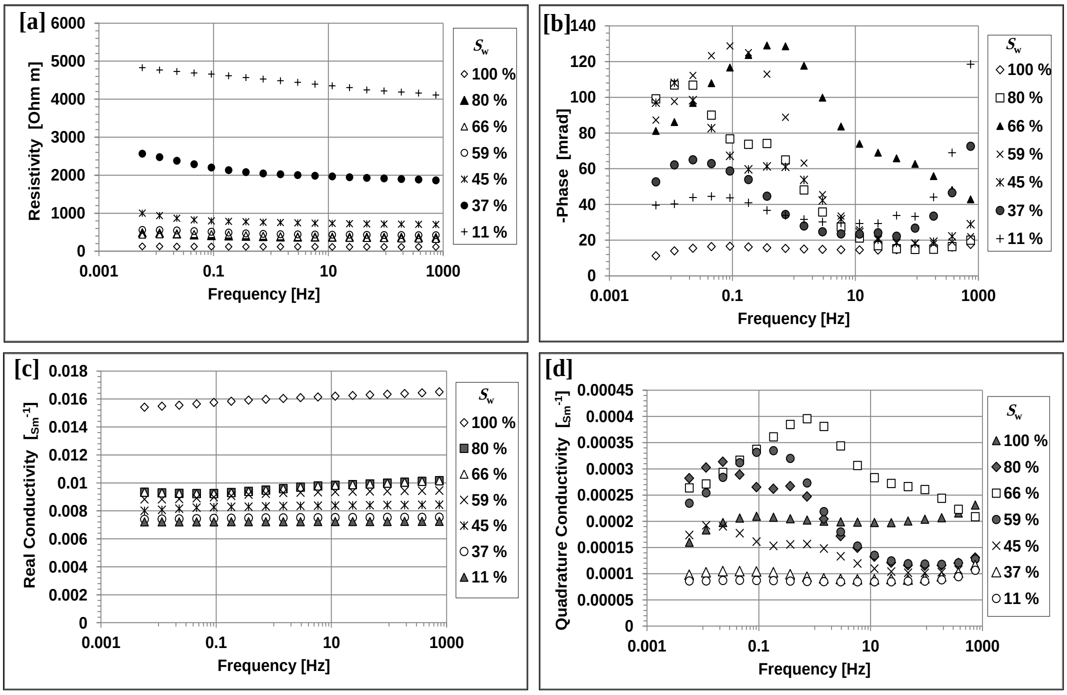

Figure (12): Frequency dependence of SIP parameters of sample T4 as a function of water saturation (Sw).

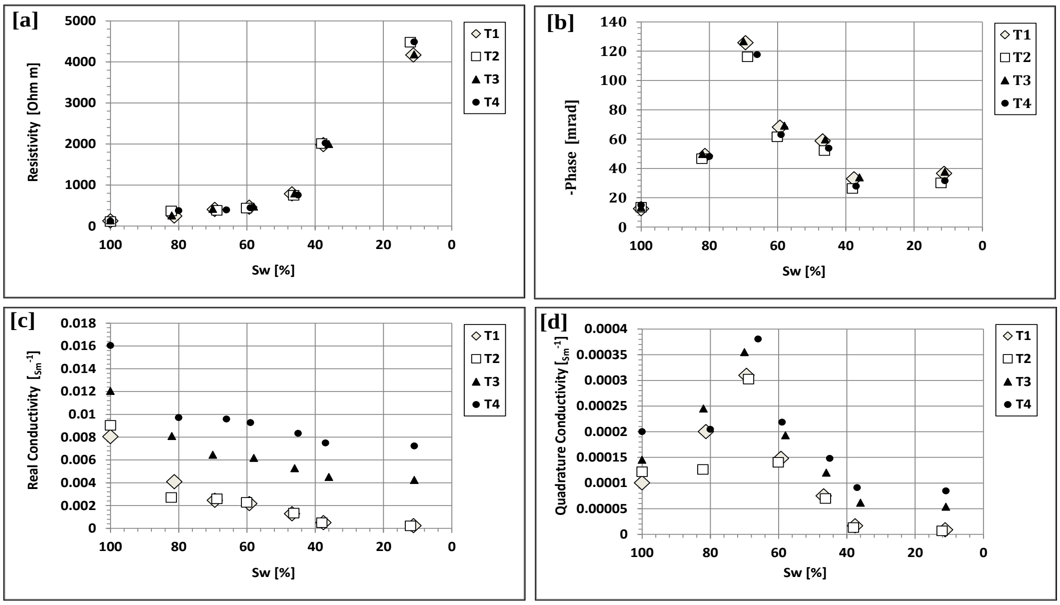

Figure (13): Dependence of SIP parameters on water saturation (Sw) at 1.4 Hz.

9. DISCUSSION

All over the study, samples with clearly flat, constant phase spectra were not observed at all. In contrast, the phase spectra of the all samples implied in this study display truly relaxation type phenomena. In fact, this study shows that, it is common for sandstones to exhibit clear electrical relaxation response over the measured frequency range used in this current study (mHz to kHz), so, it is very obvious from the shape of the resultant spectra of studied sandstones that, the Constant Phase Angle (CPA) model (constant quadrature conductivity) is totally not suitable for modelling these spectra with clear quadrature conductivity peaks. This finding agrees with the results of Scott (2004), Binley et al. (2005), Kruschwitz (2007) and Kruschwitz et al. (2010) and seems in contradiction to other previous published studies (Vinegar & Waxman, 1984; Börner & Schön, 1991; Börner et al., 1996; Pengra et al., 1999).

On the other hand, phenomenological models, such as Cole-Cole model (section 6), are more practical and commonly applied to fit the measured spectra response than theoretical ones. Although the main origin of the relaxation phenomena is not completely understood, and even some of these models are empirical and lack to theoretical physical justification (Jonscher, 1981; Ruffet et al., 1991), they still very practicable via their ability to relate descriptive petrophysical parameters of rocks to measurable spectral quantities (Pelton et al., 1983; Ruffet et al., 1991b; Dias, 2000; Kruschwitz et. al, 2010). The Cole-Cole model, which is considered the most popular model for electrical relaxations in rocks, provides a symmetrical distribution of the relaxation around a central relaxation time.

In this study, the Solver tool in Microsoft® Excel had been used to optimize the fit the electrical spectra for each sample with the 6 parameters generalized Cole-Cole model (Table 1). With the generalized Cole-Cole model, an extra parameter had been added in order to allow for the asymmetric spread of the relaxation spectra. However, due to the observed encountered asymmetry of the measured spectra with changing water saturation, fitting of the Cole-Cole model to the current spectra makes the fitted parameters highly uncertain and errors in the overall fit considerably higher than the experimental measurement errors, especially in moderate and low saturation levels.

The frequency dependence of saturated sandstones SIP response could be explained if we regard the saturated geological materials as a mixture of grains and fluids, each with different electrical conductivity. As the phenomenon of induced polarization firstly recognized as a delayed voltage response in earth materials or earth materials have the ability to store a charge similar to a common capacitor, it is always believed that the low frequency spectra response is strongly related to integrated ions diffusive polarization mechanisms.

If a saturated porous material is applied to DC voltage, the resultant current will flow via the diffusion or migration of ions across the bulk fluid saturation, grain/fluid interface and interconnected pores distribution. After the removal of the applied electric field, ions will migrate back to their equilibrium distribution. As each ion has different diffusion velocity depending upon their effective mobility and the different distances over which the ion are polarized, there will be different associated time period required for each individual ion to be fully charged.

By applying an AC voltage across saturated porous media, it is expected that the required time period associated with every ion to be fully charged will be frequency dependent. When a high frequency (short period time) AC voltage is applied across a porous media, there will not be enough time for ions to travel over their length scale. Therefore, these ions will store only small proportion of their potential charge. As the frequency of the applied AC voltage is reduced (time period is increased), greater length will be travelled by ion, a proportion of the ions will travel the full distance of their length scale, and a greater proportion of their potential charge will be stored, meaning that the stored charge increases as frequency decreases. This charge is a resistance to current flow, so reduction in the real conductivity and an increase in imaginary conductivity of the sample are expected with reducing frequency.

This can be conceptualized as a capacitor in which the current flow into the capacity reduces with increasing charge. As the frequency is reduced further, more ions will become fully charged. At a specific frequency, the time period of the applied AC voltage will be long enough for every ion to be fully charged (the capacitor is fully charged), where the phase spectra peak is observed. At very low frequency (long period time), ions with shorter charge length will begin to charge and discharge where the phase spectra start to decrease again.

Generally, the real part of the conductivity (σ') depends mainly on the saturating fluid conductivity and porosity of a porous medium, where the characteristics of the electrical double layer at the matrix-fluid interface has the major influence on the imaginary part (σ''), which explains why the quadrature conductivity is considered a more meaningful measure of the polarization magnitude than the phase angle, (Slater & Lesmes 2002; Scott, 2004; Kruschwitz et al., 2010).

The dependence of SIP measured parameters on water saturation is documented in the literature (e.g., Ulrich and Slater, 2004; Titov et al., 2004; Binley et al., 2005), however, there is no universal behavior of such impact. Moreover, even contrary relationships have been observed and reported by Binley et al. (2005). According to Kruschwitz et al. (2010), SIP relaxation curve is strongly controlled by the distribution of pore throat sizes in saturated samples, so a reduction in the relaxation curve is expected as saturation decreases. On contrary, a shift towards higher frequency and phase angle as well as quadrature conductivity for all samples with deceasing saturation to a specific point acts as reflection point, then both phase angle and quadrature conductivity start to decrease again (Figures 9-12).

Figure (13) represents a more clear and easy way to express the dependence of SIP parameters on water saturation. Similar relaxation spectra behavior with changing water saturation observed in Figures (9-12), could be more easily noticed here. Figure (13, a&c) shows the increase in resistivity and reduction in real conductivity with reducing saturation. On the other hand, in Figure (13, b&d), the non-linear behavior of both phase angle as well as quadrature conductivity with saturation is clearly observed. Moreover, the previously observed water saturation reflection point in Figures (9-12) is even more obvious here (≈70%). Another reflection point could be observer (≥ 40%).

This observed behavior could be explained as for fully saturated samples, a clear peak is noticed on both the phase and quadrature spectra that can be attributed to the existence of an effective length scale dominating the electrical polarization diffusion process. On the other hand, in the case of reducing saturation, the smaller pore throats become more and more the main dominant path controlling the relaxation process as relatively larger pores dewater faster, causing a shift in the SIP curve. That’s why; a significant increase in polarization-relaxation behavior is noticed due to bulk resistivity increase as saturation decrease. Moreover, expected further variation in the relaxation spectrum at very low saturation level will be vanished due to the major reduction in the role of large pores throats (and its effective length scale) due to dewater mechanism. These findings match of the Knight (1991) model of surface conduction, where a continuous air-water interface develops only during imbibition and breaks down at a S_w point when fluids rearrange to a more stable geometry ($S_w \approx 0.7$ in Knight, 1991).

10. CONCLUSION

The current study shows a strong dependence of SIP parameters on water saturation. Moreover, our results show that, even small reduction in water saturation away from the fully saturated statues causes result in a huge difference in SIP spectra, and its parameters. These results raise the importance and future potentiality of applying SIP measurements in studying, monitoring and modeling the vadose zone. The current study have confirmed the potential value of SIP method for groundwater modeling as well as groundwater contamination studies due to pore throat sizes and distribution influence on relaxation behavior.

Due to its sensitivity to several intrinsic parameters of the internal matrix structure of porous media (e.g. grain size distribution, pore size distribution, porosity, permeability, clay content; and saturation), SIP is considered to be one of the most promising non-invasive geophysical tool for a lot of hydrogeological studies. Moreover, greater advances would be reached by using this method to map or monitor any facies changes, solute transport or even assess the spatial variability inside one formation through surface or well-logging surveys.

Further intensive work need to be done on different sandstone types towards the optimum aim of categorizing the sandstone types depending on their physical and chemical characteristics such as clay ratio, saturating fluid conductivity, matrix and chemical composition; and pore throat size distribution, where an increase in the significance of the studied physical/petrophysical relationships could be observed.

Acknowledgement:

The authors would like to express their thanks and deep gratitude to Prof. Mohamed Mahmoud Gomaa, National Research Centre, Department of Geophysical Sciences, for his respective and valuable help and support in the conduction of the laboratory measurements.

REFERENCES

Awad, G.H. and Ghobrial, M.G., 1965: Zonal stratigraphy of Kharga Oasis. Gen. Organ. For Res. Min. 34, 77

Binley A.M. and Kemna A., 2005: DC resistivity and induced polarization methods. In: Rubin Y. and Hubbard S.S. (eds), Hydrogeophysics. Water Sci. Technol. Library, Ser. 50, Springer, New York, pp. 129-156.

Binley, A., Slater, L.D., Fukes, M. and Cassiani, G., 2005: Relationship between spectral induced polarization and hydraulic properties of saturated and unsaturated sandstone.Water Resources Research, 41, W12147.

Börner, F.D. and Schön, J.H., 1991: A relation between the quadrature component of electrical conductivity and the specific surface area of sedimentary rocks: Log Anal., 32, 612-613.

Börner, F.D., Schopper, J.R. and Weller, A., 1996: Evaluation of transport and storage properties in the soil and groundwater zone from induced polarization measurements: Geophys. Prosp., 44, 583-602.

Bücker, M., Orozco, A. F., Hördt, A. and Kemna, A., 2017: An analytical membrane polarization model to predict the complex conductivity signature of immiscible liquid hydrocarbon contaminants, Near Surface Geophysics, 15(6), pp. 547–562.

Chelidze, T. and Gueguen, Y., 1999: Electrical spectroscopy of porous rocks: a review – I Theoretical models. Geophysical Journal International, 137, p. 1-15.

Cole, K.S. and Cole, R.H., 1941: Dispersion and adsorption in dielectrics roughness of the surface and the surface charge. As the (I), J. Chem. Phys., 9, 341–351.

De Lima, O. A. L. and Sharma, M. M., 1992: A generalised Maxwell-Wagner theory for membrane polarization in shaly sands. Geophysics, 57, 431-440.

Dias, C.A., 2000. Developments in a model to describe low-frequency electrical polarization of rocks: Geophysics, 65, 43–451.

Dukhin, S.S. and Shilov, V.N., 1974: Dielectric phenomena and the double layer in disperse systems and polyelectrolytes. Wiley, New York.

Fiandaca, G., 2018: Induction-free acquisition range in spectral time- andfrequency domain induced polarization at field scale, Geophysical Journal International, p. ggy409.

Fiandaca, G., Madsen, L.M. and Maurya, P.K., 2018: Re-parameterizations of the Cole-Cole model for improved spectral inversion of induced polarization data, Near Surface Geophysics, 16, p. in press.

Fixman, M., 1980: Charged macromolecules in external fields. I. The sphere: Journal of Chemical Physics, 72, 5177–5186, doi: 10.1063/1.439753.

Gad, M.I., El Sheikh, A.E., El Osta, M.M., 2011: Optimal management for groundwater of Nubian aquifer in El Dakhla depression, western Desert, Egypt. Int. J. Water Resour. Environ. Eng. 3 (14), 393e409.

Ghorbani, A., C. Camerlynck, N. Florsch, P. Cosenza and A. Revil, 2007: Bayesian inference of the Cole-Cole parameters from time- and frequency-domain induced polarization: Geophysical Prospecting, 55, 589–605.

Ghoubachi, S.Y., 2001: Hydrogeological Characteristics of the Nubia Sandstone Aquifer System in Dakhla Depression, Western Desert Egypt. M.Sc Thesis. Faculty of Science, Ain Shams Univ., p. 260.

Gomaa M.M., 2009: Saturation effect on electrical properties of hematitic sandstone in the audio frequency range using non-polarizing electrodes. Geophysical Prospecting, 57(6), 1091-1100.

Grahame, D. C., 1952: Mathematical theory of faradaic admittance. J. Electrochem. Soc., 99:370.

Hermina, M.H, GHobrial, M.G. and Issawi, B., 1961: "The Geology of Dakhla area" Ministry of Industry, Geol. Mineral Res. Dept.., 33p., Cairo.

Jonscher, A.K., 1975: The interpretation of non-ideal dielectric Roberts, J.J. & Lin, W., 1997. Electrical properties of partially saturated admittance and impedance diagrams, Phys. Status Solidi, 32, Topopah Spring tuff: water distribution as a function of saturation, 665–676.

Joseph, S., M. Ingham and G. Gouws , 2015: Spectral Induced Polarization measurements on New Zealand sands - dependence on fluid conductivity, Near Surf Geophys, 13(2), 169-177.

Kemna, A., 2000: Tomographic inversion of complex resistivity - theory and application, Ph.D. thesis. Bochum Ruhr-Univ., Germany.

Kemna, A., A., Binley, Cassiani, G., Niederleithinger, E., 2012: An overview of the spectral induced polarization method for near-surface applications, Near Surf Geophys, 10(6), 453-468. DOI: 10.3997/1873-0604.2012027.

Kemna, A., Binley, A. and Slater, L., 2004. Crosshole IP imaging for engineering and environmental applications. Geophysics, 69, p. 97-107.

Klein, J. and Sill, W., 1982. Electrical properties of artificial clay bearing sandstones, Geophysics, 47, p. 1593-1605.

Koch K., A. Kemna, J. Irving and K. Holliger, 2011. Impact of changes in grain-size and pore space on the hydraulic conductivity and spectral induced polarization response of sand, Hydrology Earth System Science, 15(6), 1785-1794.

Kruschwitz, S., 2007. Assessment of the complex resistivity behavior of salt affected building materials, Ph. D. thesis, Technical University of Berlin, Department of Applied Geophysics, Germany.

Kruschwitz, S., 2008. Assessment of the complex resistivity behaviour of salt affected building materials: Ph.D. diss. Federal Institute for Materials Research and Testing (BAM), Germany.

Kruschwitz, S., Binley, A., Lesmes, D. and Elshenawy, A., 2010. Textural controls on low frequency electrical spectra of porous media, Geophysics, 75(4), WA113–WA123.

Leroy, Philippe and Revil, A., 2006. Induced Polarization of Glass Bead Packs with Varying Mean Grain Size, pH, and Salinities: a Review of Theoretical Models. AGU Fall Meeting Abstracts.

Leroy, P., Revil, A., Kemna, A., Cosenza, P. and Ghorbani, A., 2008. Complex conductivity of water-saturated packs of glass beads. J. Colloid Interface Sci., 321, p. 103-117.

Lesmes D. P. and Morgan F. D., 2001. Dielectric spectroscopy of sedimentary rocks. Journal of Geophysical Research, 106(B7), 13329-13346.

Mahmoud, H.H., Ghoubachi, S. Y., 2017: Geophysical and hydrogeological investigation to study groundwater occurrences in the Taref Formation, south Mut area e Dakhla Oasis –Egypt, Journal of African Earth Sciences 129, 610-622.

Maurya, P.K, Balbarini, N., Møller, I., Rønde, V., Christiansen, A.V., Bjerg, P.L., Auken, E., Fiandaca, G., 2018: Subsurface imaging of water electrical conductivity, hydraulic permeability and lithology at contaminated sites by induced polarization, Geophysical Journal International, 213, P.770–785, https://doi.org/10.1093/gji/ggy018.

Ntarlagiannis, D., Robinson, J., Soupios, P. and Slater, L., 2016: Field-scale electrical geophysics over an olive oil mill waste deposition site: Evaluating the information content of resistivity Versus induced polarization (IP) images for delineating the spatial extent of organic contamination,JournalofAppliedGeophysics,doi:10.1016/j.jappgeo.2016.01.017.

Pelton, W.H., S.H. Ward, P.G. Hallof, W.R. Sill and P.H. Nelson, 1978: Mineral discrimination and removal of inductive coupling with multi frequency IP: Geophysics, 43, 588–609.

Pelton, W., W. Sill and B. Smith, 1983: Interpretation of complex resistivity and dielectric data, Part I: Geophysical Transactions, 29, 297–330.

PENGRA, D.B., X1 L1, S. and Wong, P.Z., 1999: Determination of rock properties by low-frequency AC electrokinetics. Journal of Geophysical Research, 104, 29485-2950.

Reppert, P.M., Morgan, F.D., Lesmes, D.P. and Jouniaux, L., 2001: Frequency dependent streaming potentials. Journal of Colloid and Interface Science, 234, 194-203.

Revil A., 2012: Spectral induced polarization of shaly sands: Influence of the electrical double layer, Water Resources Research, 48(2).

Ruffet, C., Y. Guéguen and M. Darot, 1991a: Complex measurements and fractal nature of porosity, Geophysics, 137, 758-768.

Ruffet, C., Y. Guéguen and M. Darot, 1991b: Rock conductivity andfractal nature of porosity, Terra Nova, 137, 265-275.

Said, R., 1990: The Geology of Egypt. Balkema, Rotterdam, p. 734.

Schurr, J.M., 1964: On the theory of the dielectric dispersion of spherical colloidal particles in electrolyte solution: Journal of Physical Chemistry, 68, 2407–2413.

Schwarz G., 1962: A theory of the low-frequency dielectric dispersion of colloidal particles in electrolyte solution 1,2. The Journal of Physical Chemistry, 66(12), 2636-2642.

Scott, J. and Barker, R., 2003: Determining throat size in Permo-Triassic sandstones from low frequency electrical spectroscopy. Geophysical Research Letters, 30.

Scott, J. and Barker, R., 2005: Characterization of sandstone by electrical spectroscopy for stratigraphical and hydrogeological investigations. Q J Eng Geol Hydrogeol, 38, p. 143-153.

Scott, J. and Barker, R., 2006: Pore geometry of Permo-Triassic sandstone from measurements of electrical spectroscopy. In R. Barker, & J. Tellam (Hrsg.), Fluid Flow and Solute Movement in Sandstones: The Onshore UK Permo-Triassic Red Bed Sequence, 263, p. 65-81. London: Geological Society, London, Special Publications.

Scott, J.B.T., 2004: Low-frequency electrical spectroscopy of sandstone. Unpublished PhD Thesis. University of Birmingham, UK.

Shata, A., 1953: New light on the structural developments of the western desert of Egypt. Bull. Inst. Desert, Cairo 3 (1), 101e107.

Slater L.D., 2007: Near surface electrical characterization of hydraulic conductivity: from petrophysical properties to aquifer geometries - A review. Surveys in Geophysics, 28(2-3), 169-197.

Soupios, P., Kouli, M., Vallianatos, F., Vafidis, A. and Stavroulakis, G., 2007: Estimation of Aquifer Parameters from Surficial Geophysical Methods: A Case Study of Keritis Basin in Crete, Journal of Hydrology, May 2007,338,122-131,doi: 10.1016/j.jhydrol.2007.02.028.

Sumner, M. and W. Miller, 1996: Cation exchange capacity and exchange coefficient, in Methods of Soil Analysis. Part 3, Chemical Methods, pp. 1201–1230, Soil Sci. Soc. of Am., Madison, Wis

Titov, K., Kemna, A., Tarasov, A. and Vereecken, H., 2004: Induced polarization of unsaturated sands determined through Time Domain Measurements. Vadose Zone Journal, 3, Article Number. 11601168.

Titov, K., Komarov, V., Tarasov, V. and Levitski, A., 2002: Theoretical and experimental study of time domain induced polarization in water saturated sands. J. Appl. Geophys., 50, p. 417-433.

Ulrich, C., 2005: Induced polarization measurements on unsaturated, unconsolidated sands, M.S. thesis, Rutger University, USA.

Ulrich, C. and Slater, L., 2004: Induced polarization measurements on unsaturated, unconsolidated sands. (Geophysics, Hrsg.) Geophysics, 69, p. 762-771.

Vinegar, H. and Waxman, M., 1984: Induced polarization of shaly sands. Geophysics, 49(9), p. 1267-1287.

Worthington, P. and Collar, F., 1984: Relevance of induced polarization to quantitative formation evaluation. Marine and Petroleum Geology, 1, p. 14-26.